Exploring the Feasibility of Autonomous Forestry Operations: Results from the First Experimental Unmanned Machine

Pedro La Hera*, **Omar Mendoza Trejo, Ola Lindroos**
Department of Forest Biomaterials and Technology
Swedish University of Agricultural Sciences
Umeå Campus, Sweden
xavier.lahera@slu.se, omar.mendoza.trejo@slu.se, ola.lindroos@slu.se

Håkan Lideskog, Torbjörn Lindbäck, Saira Latif and Songyu Li, Magnus Karlberg
Department of Engineering Sciences and Mathematics
Luleå University of Technology, Sweden
hakan.lideskog@ltu.se, torbjorn.lindback@ltu.se, magnus.karlberg@ltu.se

Abstract

This article presents a study on the world's first unmanned machine designed for autonomous forestry operations. In response to the challenges associated with traditional forestry operations, we developed a platform equipped with essential hardware components necessary for performing autonomous forwarding tasks. Through the use of computer vision, autonomous navigation, and manipulator control algorithms, the machine is able to pick up logs from the ground and manoeuvre through a range of forest terrains without the need for human intervention. Our initial results demonstrate the potential for safe and efficient autonomous extraction of logs in the cut-to-length harvesting process. We achieved a high level of accuracy in our computer vision system, and our autonomous navigation system proved to be highly efficient. This research represents a significant milestone in the field of autonomous outdoor robotics, with far-reaching implications for the future of forestry operations. By reducing the need for human labour, autonomous machines have the potential to increase productivity and reduce labour costs, while also minimizing the environmental impact of timber harvesting. The success of our study highlights the potential for further development and optimization of autonomous machines in the forestry industry.

1 Introduction

This article presents results of using an unmanned electro-hydraulically actuated machine, which has been prototyped to carry on with fully-autonomous forestry logging operations (Lideskog et al., 2015). This machine has been developed since 2014 by the Swedish Arctic Off-Road Robotics Lab (AORO), resulting in a platform for research and development in the area of forestry machine automation (AORO: Arctic Off-Road Robotics Lab, 2021). The article's topic involves the very first results of performing a fully-autonomous forwarding task, i.e. the task of collecting and transporting logs out of the forest after tree-harvesting. To this end, the machine is able to perform autonomous navigation, object recognition and manipulation, as well as robot motion control, combination of which are essential to successfully carry on with the forwarding

operation.

1.1   Background

Forestry has come a long way from the earliest machine made from a recycled tractor to the use of sophisticated hydraulic machinery (Nordfjell et al., 2019). Among the core examples are the harvester and forwarder machines, which are the main cutting-edge industrial tools for tree harvesting in Scandinavia. Among these machines, the harvesters cut trees to small logs within the harvest area, while forwarders collect and transport them out to the roadside for further relocation. This form of operation is known as the fully mechanized cut-to-length system (CTL), a highly productive tree harvesting system, making Sweden the third largest exporter of pulp and sawn timber (Lundbäck et al., 2021; Eriksson and Lindroos, 2014).

Operating forestry machines is a demanding and difficult job (Purfürst, 2010). Yet, standard machines come equipped with old-fashioned open-loop control systems, where every degree-of-freedom (DOF) and function is individually controlled through joysticks and buttons. Therefore, the ability to demonstrate a good working performance depends on the multitasking skills of each individual operator, resulting in large productivity variation (Pagnussat et al., 2020). Apart of this, machine operators need to take thousands of multiple forest management decisions every day, while they control the machine's functions simultaneously. Over time, this cognitive load and the rough machine vibrations have a negative impact on the operators well-being, affecting also the work performance and productivity. Therefore, the interest of working as an operator has been declining in Scandinavia, making it difficult for forestry companies to recruit new qualified operators in recent years.

Research studies show that automation of forestry machines is challenging, due to the complexity of the forest environment and machine dynamics. Nevertheless, partial automation, which relieves some control of the machine from the operator's hands, has shown to be a promising technology to facilitate the work (Morales et al., 2014; Nurminen et al., 2006; Visser and Obi, 2021; Lindroos et al., 2017; Oliveira et al., 2021). As a result, machine manufacturers have recently shown an increasing interest in adopting basic automation technology, as one incremental step to boost work productivity and efficiency by making the control of machines more intuitive for operators. Examples of this adoption features the Intelligent Boom Control from John Deere, the Smart Flow and Smart Crane from Komatsu Forest, and the so-called intelligent hydraulic valves, which have given rise to the innovation of these new products (Lindroos et al., 2019; Gingras and Charette, 2017; Reitz et al., 2019; Manner et al., 2019; Technion, 2017; Komatsu Forest AB, 2017; EATON, 2019).

Due to the financial impact of forestry in the Scandinavian economy, the interest of moving towards unmanned machines for large-scale forestry operations began decades ago, at least in Sweden (Halme and Vainio, 1998; Lindroos et al., 2019). Early examples consist of radio controlled machines, such as BESTEN (eng. The Beast) (The death of the forest Beast, 2006) and the eBeaver (The radio-controlled bio-energy harvester forest ebeaver, 2011). However, machines of this kind did not meet industry's expectations, because they were difficult to remotely operate using standard open-loop control commands. Therefore, production of such machines did not reach adoption in the market. Nevertheless, unmanned machines with different levels of automation can address some of the challenges facing forestry today, including reduced soil damage, pollution, costly manufacturing, and lack of skilled machine operators (Lindroos et al., 2017; Lindroos et al., 2019). Thus, research to move from manual control to full-automation with such machines has continued since.

1.2 Literature review

1.2.1 General review about unmanned forestry machines

Automation involving unmanned forestry machines performing real forestry operations is quite rare, and very few projects exists openly available in literature. To the best of our knowledge, most relevant research projects utilize standard commercial machines from well-known brands equipped externally with portable hardware to perform tests. These developments are typically supported by machine manufacturers or forestry companies, since purchasing or owning forestry machines is too expensive for academic research. A relevant example is the excavator presented in (Jelavic et al., 2021), which uses a Menzi Muck M545 multi-purpose machine equipped with portable hardware to show some of the first autonomous abilities of a heavy-duty machine able to autonomously navigate, recognize objects and use its manipulator to do meaningful tasks. Despite not being an unmanned machine, the work of (Jelavic et al., 2021) successfully demonstrates functionalities that are required to carry on with fully-autonomous forestry operations, motivating the interest of using robotics in forestry. Although, no specific test case related to an actual logging operation has been demonstrated yet, complex tasks for construction work have been reported in (Johns et al., 2020).

Another related example is the research program Forestry 4.0 from the Canadian FPInnovations office (Automated harvesting with robots in the forest, 2020), where the aim is to automate forestry operations using robots. However, apart of small to medium size laboratory test benches, no example of a real forestry robot machine has been demonstrated so far. Similarly, the company Rakkatec produces a commercial version of an unmanned ground vehicle based on a machine once known as the RCM Harveri, an unmanned harvester machine developed in Finland (Unmanned ground vehicles for the most demanding conditions, 2021). Although the company claims that their ground vehicle can be used for autonomous operations, no demonstration of such case has ever been done.

The last example is the Ground Carriage Pully developed by the company Konrad (Visser and Obi, 2021). This was a prototype featuring a semi-autonomous/remotely operated ground unmanned forwarder to transport logs. The vehicle navigated autonomously by following the tension of a winch cable attached to it, after receiving initial commands from an operator. No complex navigation capabilities were given to this system, more than forward and backward motions in the direction of the winch cable, but it could operate in most terrains. Nevertheless, this system is not part of the company's products, and information about further development of this system is not available.

All these examples show a clear interest of the industry for machines able to perform autonomous forestry operation. However, due to the challenges related to automation of outdoor machines using robotics, real world demonstrations have not been shown so far, at least publicly.

1.2.2 Literature review about autonomous navigation in forestry

Autonomous navigation relies heavily on precise positioning information from sensors. However, obtaining this information can be challenging in harsh, unstructured, and partially occluded environments such as forest terrains.

In environments with limited GNSS signals, alternative positioning methods are often used for autonomous navigation. In forest environments, research often focuses on path planning and navigation control utilizing sensor fusion and Simultaneous Localization and Mapping (SLAM). One review study investigated positioning methods in forest environments using GNSS, Radio telemetry, Inertial navigation systems, SLAM, Bluetooth, RFID, Acoustic Positioning, bar and QR codes, and relative positioning methods (Keefe et al., 2019). In another research work, obstacle free paths were generated based on forest image data (Wu et al., 2009). In a study on GNSS denied environments, a UGV-SLAM solution was proposed based on SLAM and Shooting and Bellman methods for path planning and tracking (Fethi et al., 2018). In a recent study for unknown environments, an aerial-ground collaborative approach was considered (Zoto et al., 2020). For

a similar research problem, navigation of unmanned vehicles using a drone to identify obstacles and execute a global path planner based on rapidly evolving random trees (RRT) using dubin curves was studied (Daniel Tenezaca et al., 2020). A recent research study further proposed a path planning algorithm for partially observed environments based on Task And Motion Planning (TAMP) by using Rapidly exploring Random Graphs (RRGs) and belief space graph methods (Phiquepal et al., 2022). However, the algorithm was evaluated for an indoor partial observable environment only.

1.2.3 Literature review about computer vision in forestry

Computer vision has the potential to assist in forestry operations by enabling forest machines to perceive their surrounding environment. Although there is still no mature and widely used solution that utilizes computer vision in forestry, relevant research and experimental attempts are continuously emerging.

Specific computer vision systems have been designed for particular tasks in forestry operations, such as harvesting, forwarding, and seedling planting. For instance, conventional color cameras and machine learning algorithms have been used to detect and estimate the distance of trees near forest machines during navigation (Ali et al., 2008). Similar techniques have been implemented using LiDAR and point cloud processing (Sihvo et al., 2018).

To aid in automatic grasping of objects, researchers have used image segmentation and shape reconstruction with structured light camera data to estimate the position of logs (Park et al., 2011). Additionally, a study has explored the use of a vision system comprising a conventional color camera and machine learning algorithm for the automatic detection of spruce seedlings during planting operations (Hyyti et al., 2013).

In recent years, deep learning algorithms have undergone great performance improvements, making considerable progress in applications that include tree trunk detection (da Silva et al., 2022; Wells and Chung, 2023), tree crown detection (Roslan et al., 2020), tree separation/classification (Roslan et al., 2020; Liu et al., 2021), and tree health detection (Yarak et al., 2021; Nguyen et al., 2021). Deep learning is enabling the deployment of computer vision systems on forest machines to achieve real-time complex forestry operations. For instance, to estimate the posture of stacked logs one study used conventional color cameras and image segmentation based on deep learning (Fortin et al., 2022).

While there is currently no mature industrial application of on-site computer vision systems in forestry, research is increasingly focused on developing such systems. These systems use imaging sensors to acquire data, and corresponding algorithms are built to achieve specific functions across various operational tasks. As real-time computer vision systems become more powerful, they will likely accelerate the development of forest machine automation.

1.2.4 Literature review about crane motion control

Compared to automated manipulators, forestry cranes lack motion sensors, as they are seldom designed with having autonomous operations in mind. As a result, the necessary hardware for automation is often not readily available, making implementation of automation challenging. Therefore, forestry cranes are typically operated using joysticks that provide open-loop control commands. The operator sits in a cabin and manually controls the crane joint-by-joint, which can be unintuitive and requires strong multitasking skills for efficient operation (Purfürst, 2010; Morales et al., 2014).

Most research found on the topic of automating forestry cranes focuses on upgrading the control method from joint-by-joint to Cartesian end-effector control. This approach is more user-intuitive, as it allows the operator to control the crane's end-effector directly instead of manipulating each individual link separately. To achieve this, the crane needs to be equipped with motion sensors to implement a feedback control system for motion planning and tracking. According to literature, the most common motion planning approach used for this case is inverse kinematics (Spong et al., 2006). The work of (Münzer, 2004; Westerberg, 2014;

Hansson and Servin, 2010). showcases this solution with experimental hardware. Recent industrial examples applying this technology include the Intelligent Boom Control from John Deere (IBC), the Smart Crane from Komatsu Forest, and there are many other examples sold by consultancy firms around Scandinavia (Manner et al., 2019; Technion, 2017).

Fully-autonomous manipulation of logs is still a challenging task within the field of robotics, which is why literature on unmanned control of forestry cranes is rare. Nonetheless, two examples report experimental results of methods that could lead to fully-autonomous crane operations. The first is the work of (Ortiz Morales et al., 2014), where the authors present a motion control system for the crane of a Komatsu 830 forwarder machine. The main goal of their development was to showcase the ability to plan and control motions that resemble those of human operators. In addition, they aimed to demonstrate that autonomous control could achieve faster results compared to human operators. However, their development did not feature real world demonstrations in the forest. The second is the work of (Jelavic et al., 2021), where the authors use a Menzi Muck M545 multi-purpose machine. To control the manipulator, the authors use an adaptation of their former work introduced in (Bellicoso et al., 2016), which was later adapted for a task of piling stones in (Johns et al., 2020). However, work involving real forest operation tasks has not yet been demonstrated. Outside of academic research, there are no commercial industrial examples reported in literature, featuring any form of unmanned crane control. Nevertheless, industrial prototype machines involving this method are currently undergoing development in Scandinavia (CINTOC, 2020).

1.3   Problem Formulation

Clear-cutting of productive forests with the two-machine system has been the dominant silvicultural practice in Sweden since the 1950s (Lundmark et al., 2017). There are two particular characteristics that provide the potential for automation of forwarder machines in clear-cut operations:

1. Once the harvester machine completes clear-cutting, the paths used for to traverse the forest define the machine-trails (Hosseini et al., 2019). These routes, with minimal obstacles relative to the machine size, are sometimes pre-planned for the harvesting operation and reused by forwarder machines. The necessary digital path information is available from both the harvester data and the operation pre-plans.

2. Logs cut by harvesters are systematically piled to the sides of the machine-trails or network of machine-trails. This practice is convenient and helps minimize the time required for the forwarder to collect logs while moving through the harvesting area, given its more bulky construction compared to the harvester.

Thus, in a clear-cut scenario, the forwarder machine benefits from nearly obstacle-free paths for navigation and simplified visual recognition because logs are piled up on the ground. These characteristics have led to the hypothesis that forwarder machines could transition to full automation faster than harvester machines in forestry. To break down the overall forwarding process, the combined tasks of the operator and machine can be summarized in the following steps:

1. Navigation through defined machine-trail paths, where the information about the paths are given in digital form from harvester data or through detailed plan maps.

2. Visual log recognition along the machine-trails, done by the machine operator.

3. Decision on how to drive and stop the machine at an angle and proximity appropriate to grab logs with the crane. In most cases, an operator will place the machine in a position that allows grabbing multiple piles of logs without moving the machine.

4. Crane motion from the bunk towards the logs on the ground, coordinated through joysticks by the operator. Subsequently, the grapple is used to grab logs once the crane has reached a nearby location. Given the fact that standard grapples have a big holding area, multiple logs can be collected in one go.

5. Crane motion to carry the logs from the ground towards the bunk. Subsequently, machine operators sort the logs according to assortments, e.g. tree species and diameters, within the bunk. The sorting might not be needed, if only one assortment is collected during the given round-trip.

6. Once the bunk is fully loaded, the machine returns through the machine-trail to the unloading area, where logs are piled up for further transport.

These steps usually happen sequentially, and they are repeated until there are no more logs to collect.

Based on these observations, this article is dedicated to present our first results having the following functionalities to approach fully-autonomous forwarding tasks:

1. Autonomous navigation capabilities through via points, where the locations of these points are manually given as GPS data.

2. Log recognition using a 3D stereo camera, where the processing happens simultaneously as the machine is driving.

3. A task manager that provides the information of how to position the machine to collect logs after the visual system has identified them.

4. The crane motion control system able to autonomously collect logs from the ground to the bunk.

2 Experimental Platform

Since 2014, the AORO platform has been under development as part of different projects, including master/doctoral theses, and other research projects at Luleå University (see e.g. (Rånman, 2015) and (Lideskog et al., 2015)). The mechanical design was planned to incorporate many off-the-shelf components for hydraulics and electronic hardware, in order to reduce construction time and simplify the transition to industry. An overview of relevant hardware is given in figure 1 and described below.
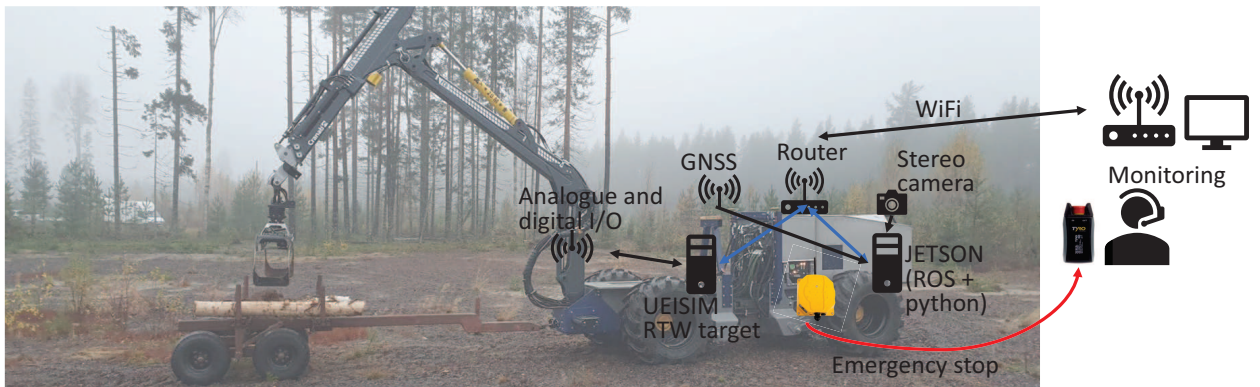

Figure 1: Hardware components.

2.1 Computing hardware

Two different computing systems are used on the AORO platform:

1. A Jetson AGX Xavier (henceforth called Jetson), with Linux as operating system, is used for the more computationally intensive tasks. This is mainly used for perception and robot loacalization due to its high GPU capabilities with respect to its size and low power usage. This uses libraries, tools and framework from the Robot Operating System (ROS) (ROS - Robot Operating System, 2021) as well as some Python programs. It also has two exteroceptive sensors directly connected via USB, which we will present later.

2. A UEISIM from United Electronics (Rack mountable Simulink/RTW target, ideal for HIL applications, 2021) is used to run most of the machine's internal control systems and to read sensors. It has a light-weight Linux OS and has several I/O cards installed for sensor inputs and control outputs. This is programmed using the built in toolboxes from MATLAB/Simulink (The Mathworks, 1990). Using Simulink Coder, models are created in Simulink and run in real-time on the UEISIM target.

These computers are interconnected via ethernet and communicates mainly via UDP messages.

2.2 Exteroceptive sensors

Exteroceptive sensors help measure the machine's relation to its environment and external objects. There exists two of these sensors in our machine:

1. The machine's position relative to the world is described by a dual-antenna GNSS connected to a national network of fixed reference stations. It is called Swepos Network-RTK and it is the Swedish mapping, cadastral and land registration authority's (Lantmäteriet's) satellite positioning support system. Having good satellite communication enables positioning of the antennas in sub-decimetre accuracy in Cartesian world coordinates. When the machine travels in dense forest terrain, other than clear-cuts, the satellite communication rapidly deteriorates to sub-metres, or worse.

2. A stereo camera, called Stereolabs Zed2, is installed at the front of the machine, pointing downwards to map the ground in front of the machine. The Zed2 stereo camera produces a plethora of sensor data, such as IMU, barometer and magnetometer data. However, so far the data we use comprise a 2D RGB image and a 2D depth map, as well as intrinsic camera data parameters.

2.3 Vehicle and Actively articulated suspension system via swing arms

The AORO platform has a front frame structure to carry the main part of the powertrain and a rear frame structure to mount auxiliary equipment. It also has a fully sensorised crane mounted on a customized subframe. The platforms are equipped with four swing arms where one end is connected to the frame and the other end to a hydraulic motor and a wheel. The swing arms thereby enable individual height control of each wheel in relation to the frame. The powertrain consists of a diesel engine as power supply with two hydraulic pumps mounted in series. One of the hydraulic pumps (variable displacement) is used to provide flow and pressure to the four hydraulic motors mounted at the end of each swing arm. This drive system is also equipped with an "anti spin" system actuated via flow valves. The other pump (variable displacement and load sensing) provides flow and pressure to the auxiliary equipment (crane in this case), swing arm cylinders, parking brake, and articulated steering cylinders, etc.
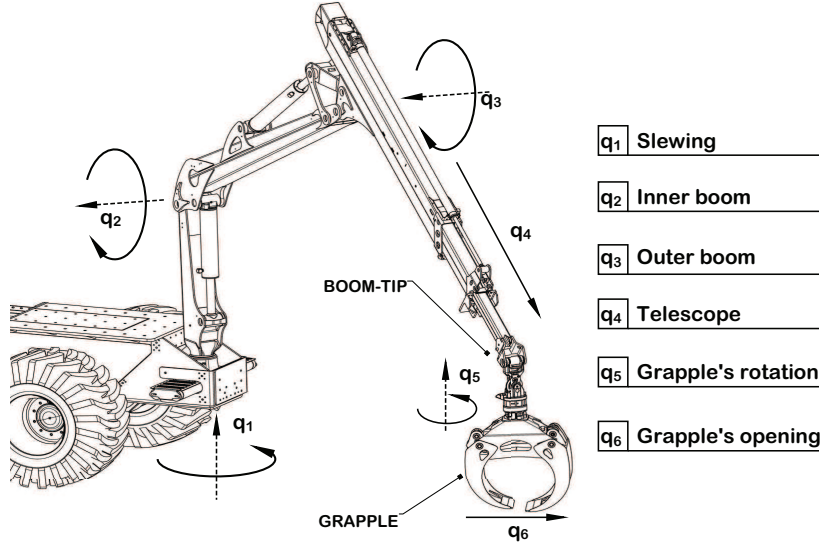
Figure 2: Forwarder crane: hydraulic manipulator with four degrees-of-freedom, specified in this graph as the slewing q_1, inner boom q_2, outer boom q_3, and telescope q_4. It holds an end-effector attached at the boom-tip, serving as a tool to grab logs. It is known as the grapple, having two active degrees-of-freedom, specified as q_5 for rotation, and q_6 for its opening. All sensors measure positive in counter-clockwise direction.

2.4 Hydraulic crane

The AORO platform uses a model FC8 crane from the company CRANAB (CRANAB FC8, 2021). This is a four degrees-of-freedom hydraulically actuated manipulator that follows a RRRP[1] configuration, according to robotics nomenclature (Spong et al., 2006). The end-effector for grabbing logs is attached at the boom-tip, model CR250 grapple, having two active degrees-of-freedom for orientation and grabbing. However, the grapple is an underactuated system, as it has no actuation at the attachment joint marked as the boom-tip in figure 2.

This crane belongs to a new line of products from CRANAB supporting the development of smart crane functions. The special feature is to have analogue encoders as joint position sensors built-in within the design. In addition, we equipped the electro-hydraulic valve with pressure sensors to measure pressure at each cylinder's chamber. Referring to figure 3, all sensors are connected to the 18-bit DAC from the main UEISIM unit. As mentioned earlier, the UEISIM is the main processor where all algorithms for motion control are implemented. Therefore, the UEISIM unit is in charge of providing the control signals to transform desired motion commands into mechanical motion by activating the hydraulic system.

3 System's functionality and methodology

As described in section 1.3, the AORO machine performs a sequential set of steps, result of which resembles tasks made with a human operated forwarder machine. The purpose of this section is to describe the system's functionality step-by-step, and consequently give a description of the methods and algorithms that are implemented on the machine to achieve the expected results.

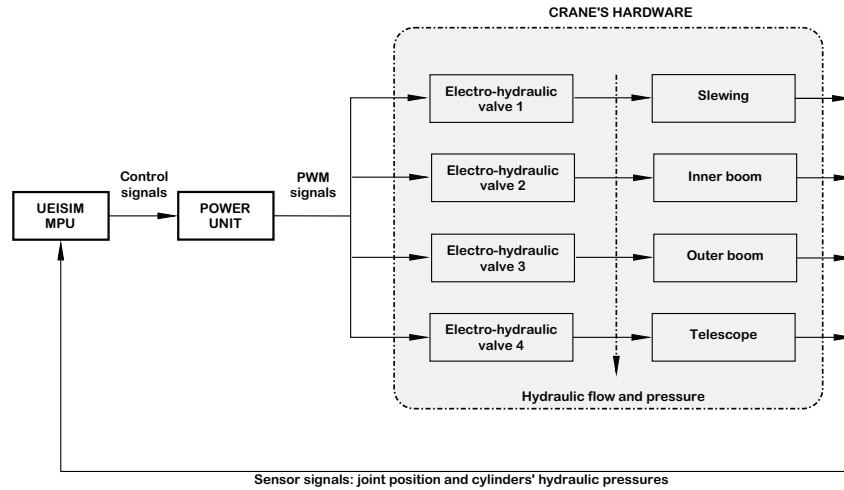
[1]R = revolute, P = prismatic.

Figure 3: Hardware architecture used as part of the crane's control system.

3.1 Functionality and limitations

Currently, the AORO platform follows a sequence of steps that repeat in a loop. Referring to figure 4, these steps and the procedure to use the AORO machine are as follows:
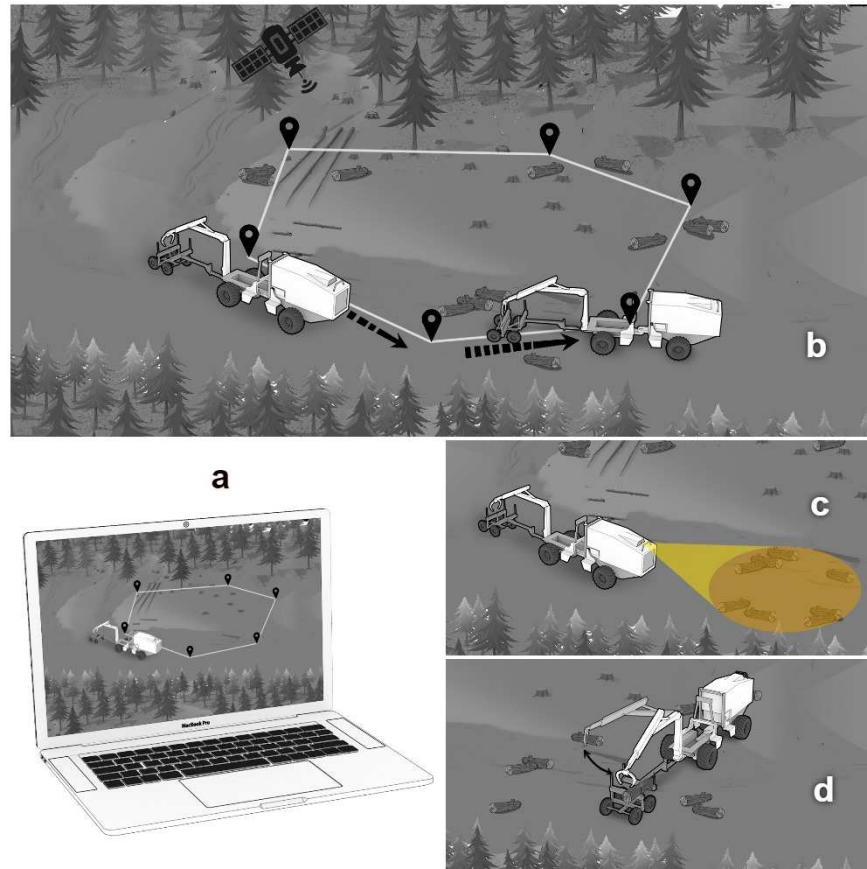

Figure 4: Sequence of steps that the AORO machine follows.

1. **Planning the mission**. Referring to figure 4a, at this stage, the human supervisor provides the route for the mission by defining GPS via points. These are set through a user interface that communicates wirelessly with the main Jetson computer. The logs to be collected lay on the ground around this route in the crane's reach.

2. **Lifting the vehicle height for navigation**. The pendulum arms for the wheels are initially on their lowest position. To initialize navigation, they are lifted up to a drivability height, in order to easily traverse the forest over medium size rocks and stumps.

3. **Autonomous navigation**. Referring to figure 4b, the machine starts traversing the forest at a constant speed of 2.3 Km/h, using GPS information, according to the plan specified initially. As the terrain refers to clear-cut, nearly no obstacles exists on these paths, apart of stumps and rocks that the vehicle can drive over.

4. **Scanning for logs**. Referring to figure 4c, the system constantly scans for logs on the ground during vehicle navigation, using the stereo camera placed in front of the machine.

5. **Stopping the vehicle when logs have been found**. Once a log or groups of logs have been found, the machine shortly stops at a distance of 4 meters to get a better visual recognition and positioning of the logs. This information is then translated to the machine's coordinate system, which is used to provide coordinates to the crane's motion control unit.

6. **Placing the load bunk for collection**. At this stage, the vehicle travels an average distance of 5 meters passed the logs, and stops at a distance where the logs lay almost next to the load bunk. This facilitates the crane's tasks, by minimizing the crane's distance of travel. When several logs are found, the system stops at a distance where the crane will be able to reach all logs in a nearby area without the necessity to move the vehicle.

7. **Lowering the vehicle**. At this stage, the vehicle height is lowered to its minimum range to have a lower center of gravity and better stability when the crane is moving and carrying logs.

8. **Collecting logs**. Referring to figure 4d, at this stage, the crane's motion control system plans the necessary trajectories to reach the logs and load them into the load bunk. From this point, the sequence starts all over again from step 2 and ends when the last via point is reached or by manual means.

As this project is undergoing development, there are certain limitations in the system's current functionality that are worth mentioning:

- The plan for the operation needs to be inserted by a human supervisor using GPS via points. Communication between a harvester machine and our machine is work in progress.

- When the machine stops to collect logs, there is currently no camera on the crane to observe the logs on the ground. Therefore, the accuracy of the crane's work currently depends on the correctness of the log position estimation using the camera mounted at the front of the machine.

- The sequence of steps is repeated until the last via point is reached or by a human operator that stops the system. Currently, the system does not have a method to estimate when the load bunk is full.

- Currently, the system is only capable of loading the load bunk, but not the reverse task, as this is still challenging not having a camera dedicated to the crane.

3.2 Methods and algorithms

The algorithms required to perform the tasks described above have been divided into actions that are supervised and commanded through a task manager. The activity manager provides the required flags to switch between each action, such that two actions cannot happen simultaneously.

The main functions implemented on the AORO platform are the following:

- **Autonomous navigation**, in which the machine is able to navigate by specifying via points.

- **Autonomous log recognition**, in which the machine is able to use its vision capabilities to observe logs laying on the ground, and defining their location according to the machine's reference frame.

- **Autonomous crane motion control**, in which the machine is able to use its crane to collect the logs that have been recognized by the vision system.

The overview of the algorithms and the description of the task manager that sequentially switches among them is given below.

3.2.1 Navigation Control

The machine navigates between an initial and a final destination by following a trajectory that connects GPS waypoints. In this study, we adopted a straightforward approach based on the direction of the machine's front end. The algorithm calculates the difference between the bearing of the current waypoint and the heading of the machine's front end, and feeds this information into a P controller that determines the desired rate of steering angle. The controller then sends this information to a hydraulic valve that controls the cylinders that adjust the articulation angle. When the machine approaches a certain distance from the via point (based on the machine's steering radius), it switches to the next.

3.2.1.1 Robot Localization

The robot localization node utilises built-in functions and packages from ROS to create a real-time kinematics model of the machine using kinematic equations (see figure 12). First, an XML file is composed where basic geometry, all links and joints are described. Then, feeding sensor data as input to the localization node, rigid transformations define the position of each degree-of-freedom at each time step.

3.2.2 Vision System

At the moment, the objective of visual perception is to enable fast-enough log detection, so that position coordinate outputs can be used in subsequent crane control. The visual perception runs in ROS and contains two nodes. The first is called DNN and comprises a deep neural network used for real-time object recognition. The second is referred to as Vision, comprising the data evaluation of detected objects where logs are extracted and positioned in absolute terms.

For the DNN node we use a modified version of the Legged Robotics ROS package called darknet_ros (YOLO ROS: Real-Time Object Detection for ROS, 2021), which comprises a real-time object detector named YOLOv3 built within a neural network framework named darknet (Darknet: Open Source Neural Networks in C, 2021). Darknet-53 performs well for our purpose, at the time of testing working twice as fast with the same classification accuracy for comparable nets (Lawal, 2021). This is an important property given the necessity of real-time execution. At the time for full testing, YOLOv3 had shown substantial
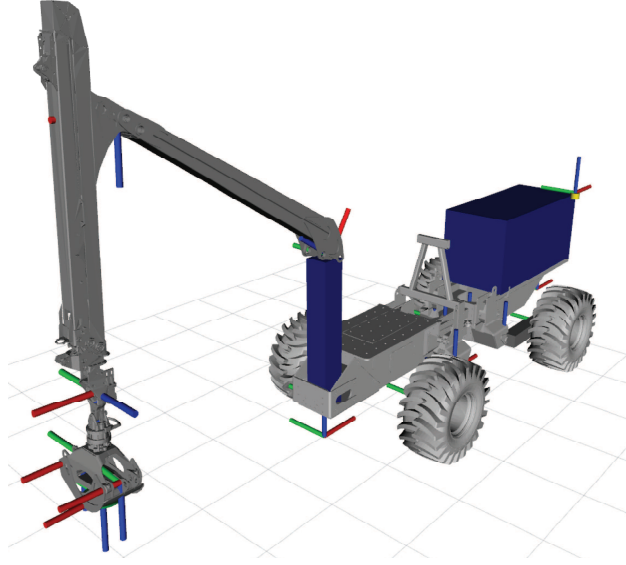
Figure 5: AORO robot joint and link definitions graphically depicted in Rviz (3D visualization tool for ROS applications).

improvement compared with earlier versions (Farhadi and Redmon, 2018) and had ROS integration. The detector was previously tested in forestry applications (Li and Lideskog, 2021).

3.2.2.1 DNN node: Data collection, labelling and augmentation

To train the neural network in the DNN node, RGB data was collected at the forest area to be used for forwarding demonstrations and experimental validation.

Image data was collected using the stereo camera Zed2 with a resolution of 1280x720 pixels. To this end, we manually moved the camera by hand in an area of 75x75 metres where logs had been strategically dispersed to represent different placements and orientations. The weather was sunny with a slight overcast, producing shaded parts on the grounds. No rain had fell for days and the grounds were dry. That enabled the opportunity to ensure data was collected both having the sun at the back and front facing the camera. Logs were also dispersed in both shaded and sunlit areas, as well as areas with and without vegetation. The logs consisted of birch trees with a mean diameter of 25 cm and a length of 2 m. Images were captured so that distance and angle to logs were differed to ensure images spanned the entire range of possible encounters for a machine in that area (see figure 12). Only birch logs were used in all images, ensuring no confusion with other tree species (apart from standing trees). In total, 1700 images containing over 3500 annotated logs were captured and used as a training and validation data set.

A common step to increase the robustness of an object detector working on RGB imagery is to augment the training dataset by adding copies of already existing data, but having them slightly modified in terms of e.g. brightness and contrast. That alleviates over-fitting when training the detector and acts as a regularizer (Shorten and Khoshgoftaar, 2019). The original dataset was augmented with modifications in image rotation, saturation, exposure, blur and noise, increasing the total dataset size to 6300 images of which a major part of 95% was used for training and the rest for validation.

Figure 6: Examples of labelled images from test site where data was recorded, and subsequent demonstration and experiments were performed.

3.2.2.2   DNN node: Preparing the dataset for training

The dataset was resized to 608x608 pixels, where black edges over and under the image ensured the correct ratio. This image size is specifically tailored to suit the training process for our choice of neural network.

The ROS package darknet_ros was also used for training, with a neural network having 53 convolution layers, named Darknet-53. Within Darknet-53 the encapsulated YOLOv3 has a training process that reflects the original YOLOv3 algorithm. By feeding the training set into Yolo-ROS, we can get a so-called weights file trained on the prepared data. A weights file is a binary file containing the parameters for the 53-layered neural network. With transfer learning, we utilized a pre-trained model that was previously trained on logs as objects, building on a source data set of approximately 1000 images. Our final weights file achieved a mean average precision (mAP) of 80.51%, which is an evaluation metric (Salton and McGill, 1983) commonly used in the PASCAL Visual Object Class (VOC) challenge (Everingham et al., 2010). The input image size to the network were 608x608 pixels, momentum was set to 0.9 and initial learning rate to 0.001. Decay was set to 0.0005 and the training steps to 3200 and 3600.

3.2.3   Vision node

The vision package encompasses the log positioning algorithm, which uses input from the stereo camera depth map and input from the DNN as bounding box positions to calculate and publish log positions relative to the camera coordinate system.

Positioning detected objects in relation to the camera (and thus the machine itself) is conducted as follows. After target objects are recognized by the DNN node, the corresponding depth map of the area and corresponding bounding box 2D image coordinates are fed into the vision node. The depth information within the bounding box is used to calculate the actual position of the object. We use the mean value of depth data in an area of 8x8 pixels within the bounding box center to calculate the object depth, which significantly increases calculation robustness, but may add a few milliseconds to the calculation time. Furthermore, this is a viable method since the camera is directed downwards and to a great extent depicts terrain areas and not areas that otherwise would rapidly change.

Using the model of a pinhole camera (Forsyth and Ponce, 2003), the relationship between the coordinate of a 3D space point [X, Y, Z] and the pixel coordinate of its image projection in 2D [u, v] is given by:

$$Z \begin{bmatrix} u \\ v \\ 1 \end{bmatrix} = \begin{bmatrix} f_x & 0 & c_x \\ 0 & f_y & c_y \\ 0 & 0 & 1 \end{bmatrix} \cdot \begin{bmatrix} R & t \end{bmatrix} \cdot \begin{bmatrix} X \\ Y \\ Z \\ 1 \end{bmatrix} \tag{1}$$

where R and t denotes rotation and translation, which relate the world coordinate system to the camera

coordinate system, f_x and f_y are the camera's focal length in X- and Y-axis, and c_x and c_y are the center of the camera's aperture. Equation (1) gives that

$$\begin{bmatrix} X \\ Y \end{bmatrix} = Z \cdot \begin{bmatrix} (u - c_x)/f_x \\ (v - c_y)/f_y \end{bmatrix} \tag{2}$$

If the pixel coordinate (u, v) and the depth information of the pixel Z is known, the actual spatial position represented by the corresponding pixel can be calculated according to the camera parameters f_x, f_y, c_x, and c_y, which are usually provided by the camera manufacturer.

3.2.4 Active suspension height control

To set the vehicle height, a reference height is sent from the activity manager to the swing arm control system. This reference value is then used to control each swing arm hydraulic cylinder individually. To this end, a proportional controller is used to generate the control signals for the hydraulic valve of the swing arms' cylinders.

To improve the machine's navigation, the vehicle is equipped with passive suspension through float control valves. These valves can be activated on either the front or rear axle, but never on both simultaneously to prevent the vehicle from tipping over. When activated, the swing arm cylinders on the left and right sides are cross connected, i.e. the inlet port on one cylinder is connected to the outlet port on the other, and vice versa. This causes the cylinders to move simultaneously in opposite directions, thus keeping the ground pressure equal on both sides, similar to a beam axle on a car. The float configuration is activated just before the machine moves for drivability and deactivated during the log loading operation for stability.

3.2.5 Crane's motion control system

Controlling heavy-duty hydraulic manipulators is challenging. Some of the main reasons are the unpredictable loads and nonlinear dynamics, which include large amounts of residual vibrations resulting from oil compressibility and mechanical flexibility (Manring, 2005).

Our research group has been involved in the development of automation technology for forestry cranes for nearly two decades. Therefore, the motion control algorithms applied in the AORO platform are modifications of former work, some of which is presented in (La Hera and Morales, 2014; La Hera and Ortíz Morales, 2015; La Hera et al., 2021) and references therein. In short, the reference tracking feedback controller is a nonlinear controller using sliding mode control, giving robustness to unmodeled dynamics and disturbance rejection. In addition, this control strategy allows to attenuate residual vibrations, a common problem from the crane's dynamics behaviour. The validation of the performance of this type of control system has been presented in (La Hera and Ortíz Morales, 2015).

To plan motions, we use Dynamic Movement Primitives (DMP), following the machine learning algorithm detailed in (La Hera et al., 2021). This approach is based on the concept of learning by demonstration, in which we manually demonstrate point-to-point motions to the crane, following quasi-parabolic paths, as those used by professional machine operators. This is done using joysticks. Consequently, the crane is able to use these demonstrations to dynamically plan any point-to-point motions from an initial to a desired position, mimicking the characteristics of the demonstrated motions.

The algorithm to control crane motions is sequentially executed once the activity manager has sent a trigger command. This trigger command results from successfully recognizing a log on the ground and getting its Cartesian location, as well as stopping the machine at a preplanned distance to collect the log. The input to the algorithm is the position of the logs in Cartesian Coordinates, according to the crane's reference frame. Consequently, the algorithm plans crane trajectories from the bunk to the side of the vehicle where the logs

are located. The grapple opens during this motion. Once the target position is reached, the grapple closes and holds the logs. The reverse of this sequence is executed to load logs into the bunk. A pseudocode giving an idea of how the algorithm works is presented in algorithm 1.

Algorithm 1 Motion planning based on DMP

Input: Location of logs given in Cartesian World Coordinates [X,Y,X] and rotation ϕ
Output: Joint reference trajectories $q_{i_{ref}}(t)$ where $i = [1, 2, 3, 4, 5, 6]$
1: **procedure** MOTIONPLANNING
2: *From bunk towards log*:
3:     **if** $trigger\_signal = 1$ **then**
4:         $[q_{1_{ref}}, q_{2_{ref}}, q_{3_{ref}}, q_{4_{ref}}] = DMP\_Algorithm(X_{target}, Y_{target}, Z_{target})$
5:         $[q_{5_{ref}}, q_{6_{ref}}] = OpenGrapple(\phi_{target})$
6: *From the sides towards bunk*:
7:     **if** $(target\_reached = 1)$ & $(grapple\_closed = 1)$ **then**
8:         $[q_{1_{ref}}, q_{2_{ref}}, q_{3_{ref}}, q_{4_{ref}}] = DMP\_Algorithm(X_{bunk}, Y_{bunk}, Z_{bunk})$
9:         $[q_{5_{ref}}, q_{6_{ref}}] = OpenGrapple(\phi(0))$
10:     $finished\_sequence = 1$.

3.2.6 Activity Manager

To control different activities and monitor progression towards achieving the mission, an activity manager was developed using Simulink Stateflow and integrated in the main Simulink software structure (The Mathworks, 1990). The structure of the activity manager is presented in Figure 7 and it is divided into the two main states "Idle" and "Auto" where the default transition Td_1 is set to "Idle". The transition between "Idle" and "Auto" is controlled with a switch. This enable start and stop of the automation process manually via a remote control and also from the path tracking system when the mission has been completed, i.e. when the final via point has been reached, or when an operator has manually stopped the mission.
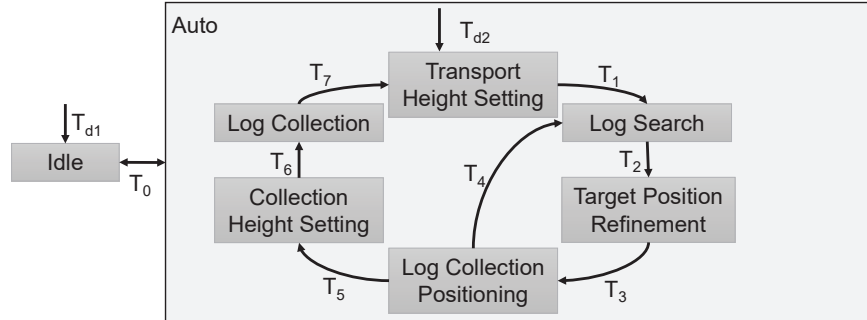

Figure 7: Structure of the Activity Manager.

The autonomous forwarding mission is divided into six states with transitions in-between (see Figure 7). When entering the Auto-state, a default transition Td_2 is set into a state with the objective to set the vehicle height to a suitable transport level (the "Transport Height Setting" state). The activity manager sends a set-height to the pendulum arm control system (outside the activity manager see Figure 8), which then independently adjusts the pendulum arms until the set-height is reached. This triggers the transition into the "Log Search"-state T_1. In "Log Search", the drive control system is activated and the vehicle starts following the predefined path. As previously stated, note that it is assumed that the path follows a strip-road from the harvester track and that all logs to be picked up can be reached from this path.

During navigation, stereo camera information of the surrounding is gathered via the perception system and
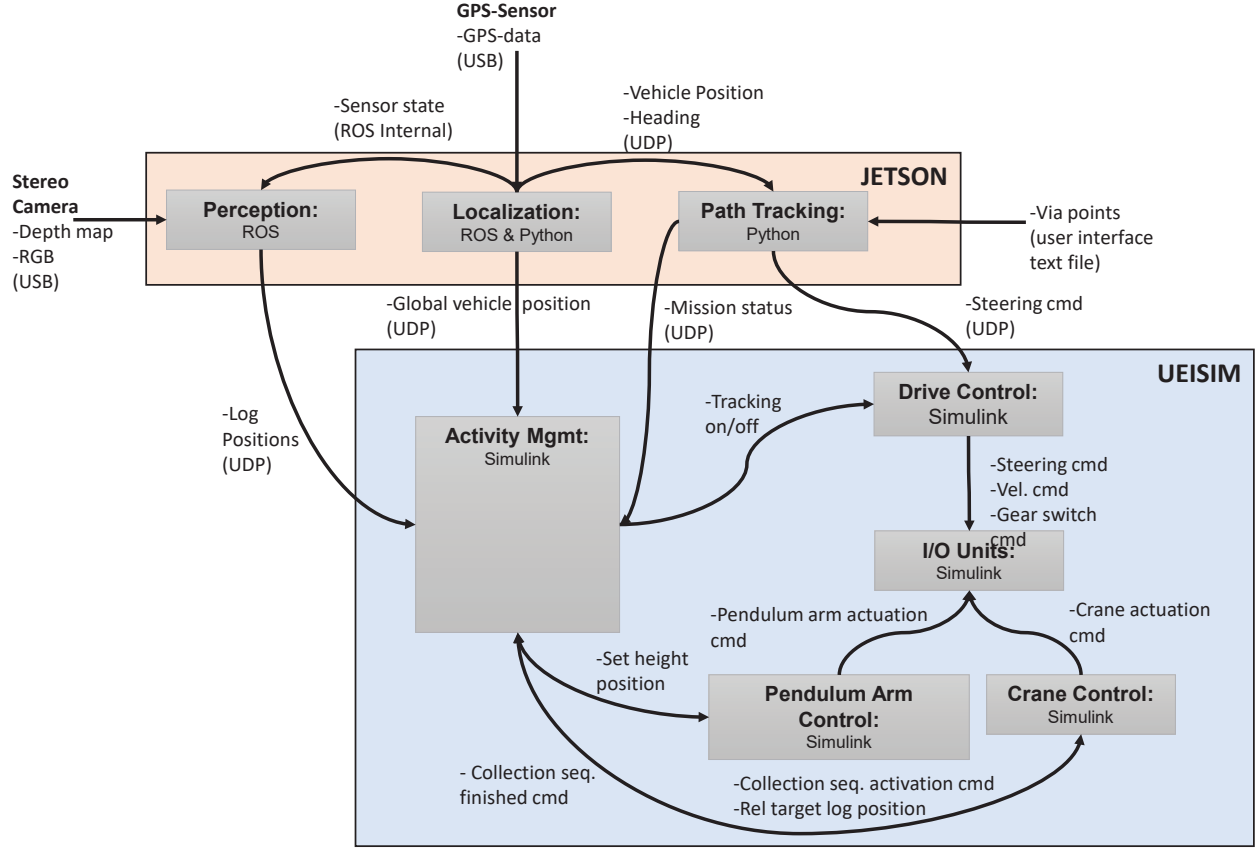
Figure 8: Activity Manager Software Architecture.

used to continuously store floating mean values of the identified log positions. In addition, based on the GNSS-position of the vehicle given by the localization system, the distance between the crane reference frame and the closest log is calculated. When this distance is below a threshold $\delta > \epsilon > 0$, the closest log is set as the target log and the transition into "Target Position Refinement"-state T_2 is triggered. To improve the positioning accuracy, the tracking system is deactivated, i.e. the vehicle is stopped and then the detected log positions are updated. After a predefined hold-time, transition T_3 is triggered where the "Log Collection Positioning"-state is entered. For collecting the logs, the crane's reference frame should be positioned at a certain range and ahead of the target log. This is achieved by using a circle with origin at the target position and a predefined radius. The tracking system is activated and the position of the crane foot in relation to the target log is then monitored to ensure that the crane foot first enters the circle. Then, as the crane foot exit this circle, the tracking system is deactivated and thus, the vehicle stops.

At this stage, a validity check is performed by evaluating that the target log position is realistic in the local crane coordinate system (used for the log collection). If not, the transformation T_4 back to "Log Search" -stage is triggered. Otherwise, the system transit into the "Collection Height Setting"-state T_5. At this stage, to improve the load capability and machine stability, a low set-height is sent to the pendulum arm control system, which independently adjusts the pendulum arms until the set-height is reached and then trigger the transition into the "Log Collection"-state T_6. Now the target log position relative the crane foot is sent to the crane control system, which generates local crane trajectories (including the grapple). These trajectories are used to control the actual crane movements. When the collection procedure is finished, a command is sent to the activity manager that transits back to the initial "Transport Height Setting"-state. This state-transition behaviour loops until the mission has been completed.

4   Testing scenario

The tests to present our results were planned in two stages. In the first stage, the intention is to evaluate the performance of each individual component involving autonomous navigation, log recognition, and crane motion control. In the second stage, the intention is to evaluate whether the task manager is capable to combine these methods to perform a fully autonomous forwarding task.

4.1   Tests for the individual system's functionality components

4.1.1   Testing the autonomous navigation control system's performance

Tests were performed to verify the machine's ability to autonomously navigate by defining via points in GPS format. These tests consisted on defining a rectangular path given by four via points (see figure 11), and letting the machine traverse this route for four consecutive laps. To test the robustness and converge to the desired path from different initial conditions, the machine's initial position was changed for each new test sequence.

4.1.2   Testing the crane's motion control system's accuracy

Tests were performed to verify the performance of the crane's motion control system and to calculate an estimation of its accuracy. These tests consisted on performing automatic motions from an initial configuration towards different desired goal locations in the world coordinate system (Cartesian coordinates), in order to calculate the deviation at the final position. The initial configuration was the center of the trail where logs are piled up (see figure 9). The goal location referred to the desired Cartesian coordinate target where the crane's tip was meant to reach. Referring to figure 9, four desired test locations were selected to cover the four quadrants in the x-y axis, having the coordinate system at the base of the crane.
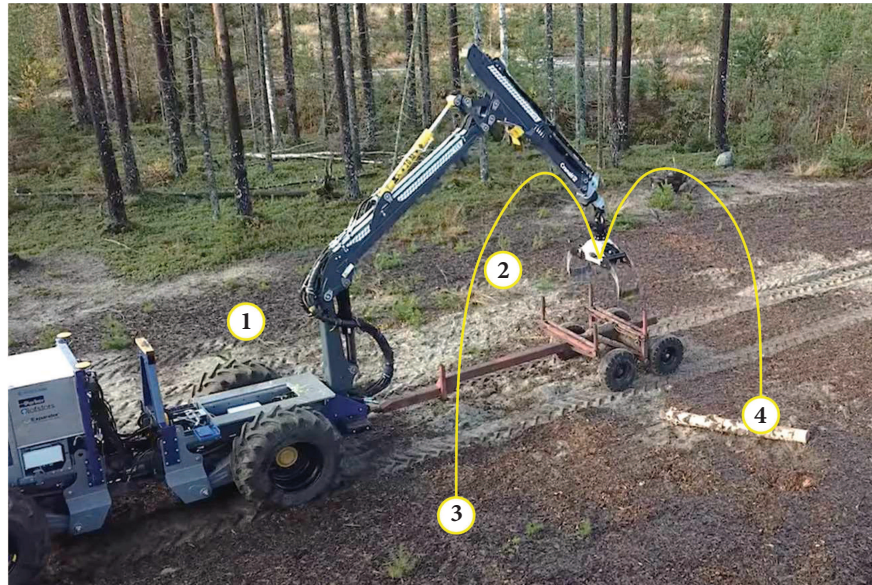

Figure 9: Crane's desired motions from it initial configuration at the center of the trail, towards four desired locations in the Cartesian Space.

To calculate an estimation of the positioning accuracy, the deviation of the crane's tip position to the desired target was calculated by Euclidean distance. To calculate the tip position, we used the forward kinematics

presented in (La Hera et al., 2021). To get a reliable estimation, several repetitions of the same motion to each target location were performed. Consequently, the mean value for all the deviation errors of the four target locations was used to get a final estimation of the crane's positioning accuracy.

4.1.3   Testing the logs' location algorithm accuracy

Tests were performed to calculate the accuracy of the log recognition algorithm. These tests consisted in estimating the location of logs that were manually placed on the ground at specified known locations. To this end, the test consisted on placing two logs, five meters apart from each other, according to the reference frame presented in figure 10. The logs were placed according to the following characteristics:

1. In the first instance, the logs where placed at zero degrees, specified by the reference system observed in figure 10. In this position the machine has the highest visibility to the whole log, as the direction of travel is perpendicular to the logs.

2. In the second instance, the logs were placed at 45 degrees of rotation. In this position the machine observes the logs at an angle.

3. In the third case, the logs were placed at 90 degrees of rotation. In this position the machine has the least observation of the logs, as the direction of travel is parallel to the logs.

For each of these cases, the machine started autonomously driving from a distance of 40 meters away from the first log (see figure 10 for reference).
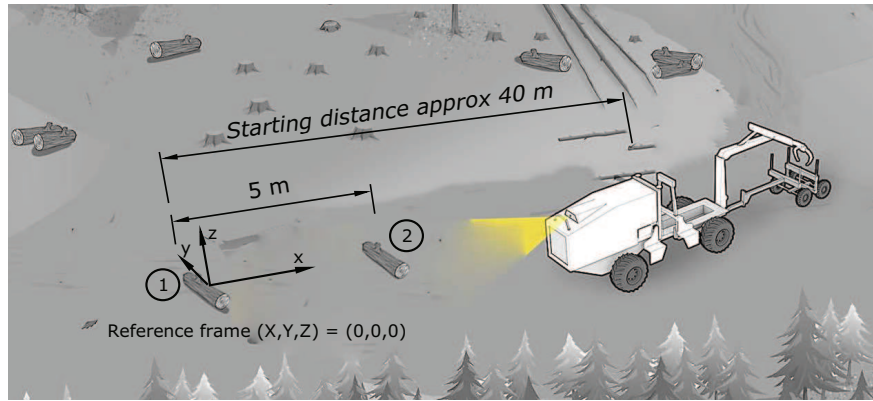

Figure 10: The setup to test the log recognition accuracy. Two logs are placed on the ground, five meters apart. The machine starts autonomously driving from 40 meters, giving estimations for both logs as it goes.

The log recognition software provides 15 estimations per second according to the machine's main reference system. Consequently, this data is transformed into different reference systems to, for example, provide logs' location coordinates to the crane control system, or to navigate the vehicle to better position itself when collecting logs. In these particular tests, the data was transformed into the world coordinate observed in figure 10.

The purpose of the estimation is to give the coordinates of the center of the logs, as this is the value that is transferred to the crane's motion control system. To get a reliable estimation, several repetitions were performed to obtain an averaged value of the recognition software accuracy. Consequently, we measure the deviation of the estimation to the values measured by hand using Euclidean distance. The deviation from true values gives us an estimation of the recognition software accuracy.

4.2 Testing the complete forwarding task

The experimental scenario refers to the location where the AORO machine was unveiled to the public, which is also the place where we performed experimental tests (The world's first self-propelled forestry machine, 2021). It is a region in the northern county of Sweden belonging to one of our industry partner, with the closes city being Hörnefors. The specific coordinates of the site in the WGS84 decimal (lat, lon) system is $63.657853, 19.895562$. Referring to the left side of figure 11, the testing area had a length of 40 meters and width of 30 meters.
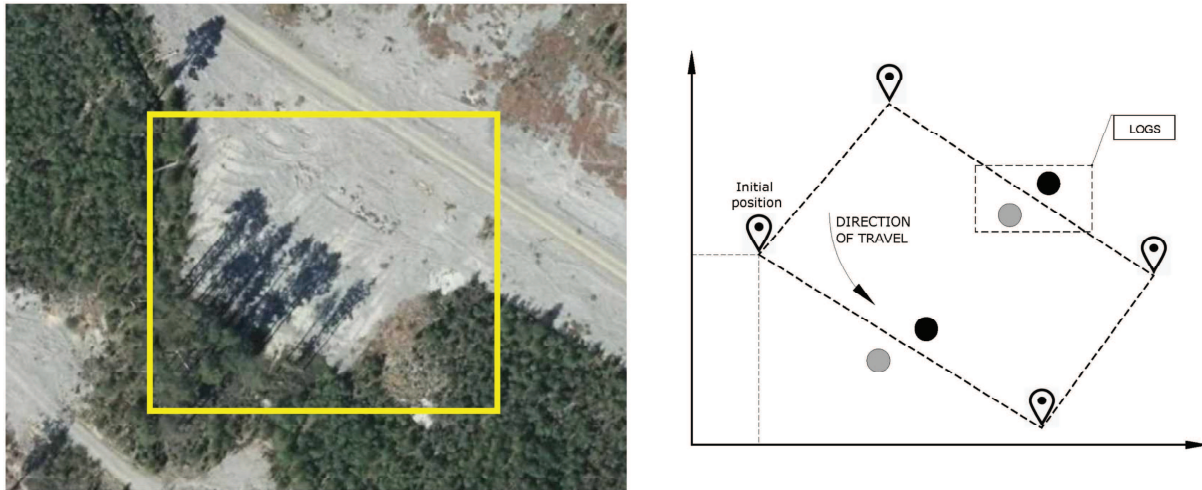

Figure 11: **Left:** Forest site where the experiments were carried out. The square points to the particular area for the experiment. **Right:** The mission planned for testing the machine's ability to carry on with fully autonomous forwarding.

The experimental testing was designed according to the following mission:

- Referring to the area marked in yellow in the left side of figure 11, four GPS via points sufficed to define the mission path (see right side of figure 11). These points were inserted manually and communicated to the main machine's computer wirelessly.

- As shown in the right side of figure 11, logs were placed manually on the longer sides of the routes, either to the right or to the left of the main path. As explained in section 3.2.2, only birch logs were used in these tests, because this is a common species for commercial harvesting in Sweden and possibly easy to recognize.

- Each time the machine passed through the longest sides and collected the logs, they were immediately replaced by other logs for the next time the machine would pass through.

- Referring to figure 9, a trailer was attached to emulate a forwarder machine. The dimensions of the trailer were added to the recognition software, in order to have the coordinates required for the crane to release the logs it picked up from the ground.

4.2.1 Precision measurement

To assess the entire system's precision with an external measuring tool, we used a mobile two-camera setup. For each position a log was recognized and targeted by the system, two images were taken. We chose to program a short pause in the crane's movement towards the log, stopping for a second on top of the log just before activating the grapple and grabbing the log. That enabled the cameras to record an image frame each

in the machine rear end's longitudinal and transversal direction. With knowing the grapple true size, each image was given a measurement scale and thus a measure from the grapple's ideal grabbing point and the log's centre point was determined. No rounding of measures has been done in the resulting values; however at least a $\pm$ 2 cm error is to be expected.

5 Experimental results

5.1 Results for the individual system's functionality components

5.1.1 Navigation Control

Referring to the mission plan presented in figure 11, the initial experiment verifies the machine's ability to navigate by defining via points. To this end, the machine was started from different initial conditions, in order to validate the convergence of the motion towards the shortest path needed to traverse the terrain by directly connecting the four via points, i.e. in a rectangular path.
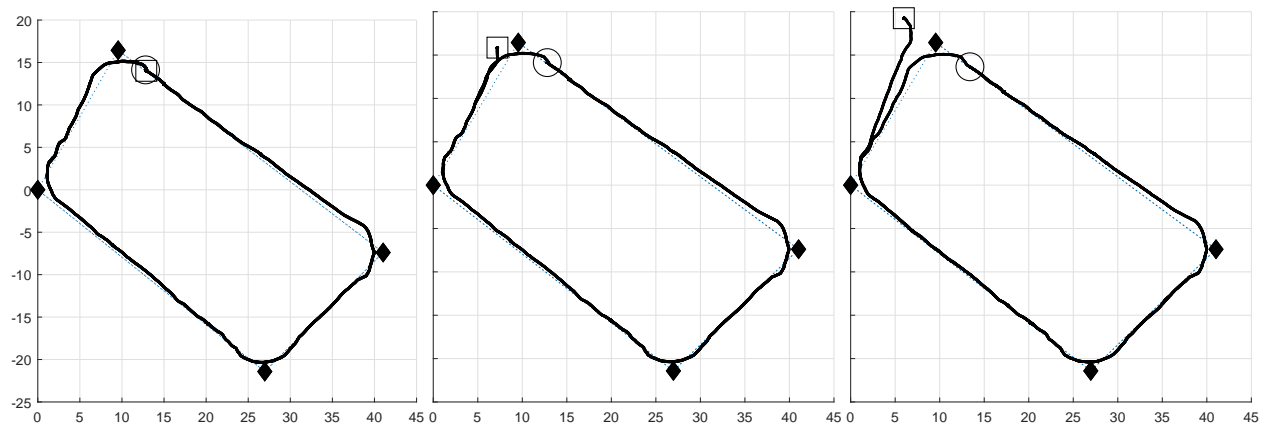

Figure 12: Examples of running the navigation control system from three different initial conditions. The square markers point at the initial conditions, while the circular marker point at to the final position. The four via points are plotted with back diamond shaped markers. The units in these graphs are in meters.

Figure 12 shows three of the results from these tests, having the square and circular markers pointing at the initial and final locations of the machine respectively. In all these cases, we let the machine run for two laps to verify that the motion converges towards the desired track. In figure 13, we show the results of six test cases superimposed on the same image, which clearly shows that the machine's autonomous navigation control system is able to converge towards the desired route, despite starting at different initial conditions.

5.1.2 Logs' recognition

Referring to the tests described in section 4.1.3, figure 14 shows results from the log recognition algorithm. From left to right, the three plots in figure 14 refer to the cases where the logs are placed a) straight to the camera, having the highest visibility of the log, b) at 45 degrees angle, where the camera observes the log at an angle, and c) at 90 degrees angle, where the camera would have the least visibility of the log.

As the system is able to provide 30 estimations per second, our software uses the averaged value to give a final estimated result. Figure 15 shows results using a histogram for the log marked as two in figure 10. From left to right, the histograms in figure 15 represent the cases a), b) and c) described above. The bars on
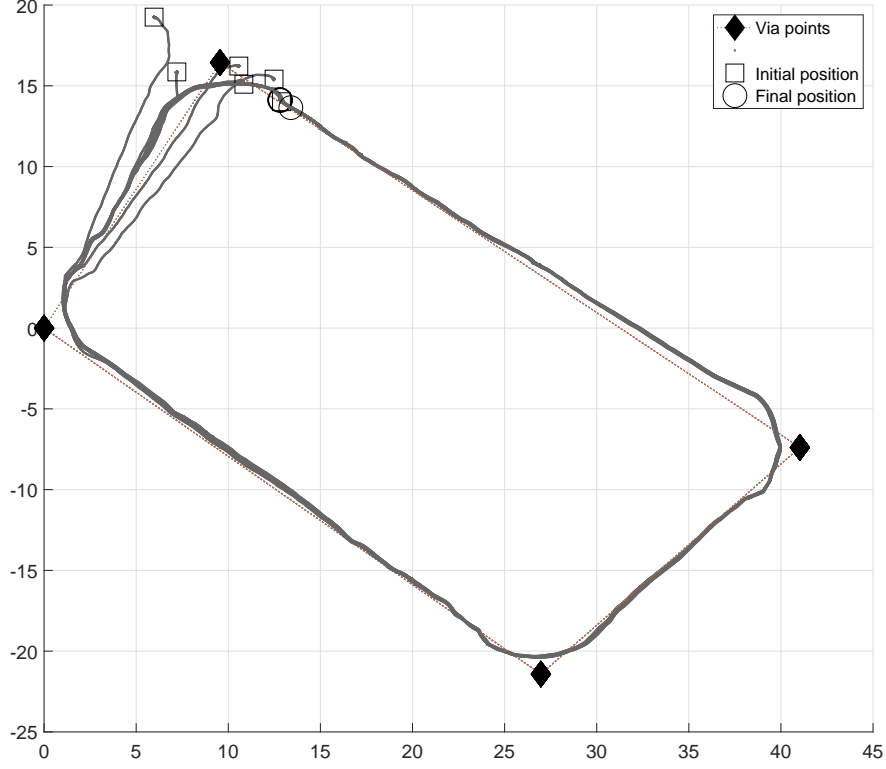
Figure 13: Results of the navigation control system for six different test cases. The square markers point at the initial conditions, while the circular marker point at to the final position. The four via points are plotted with back diamond shaped markers. The units in these graphs are in meters.
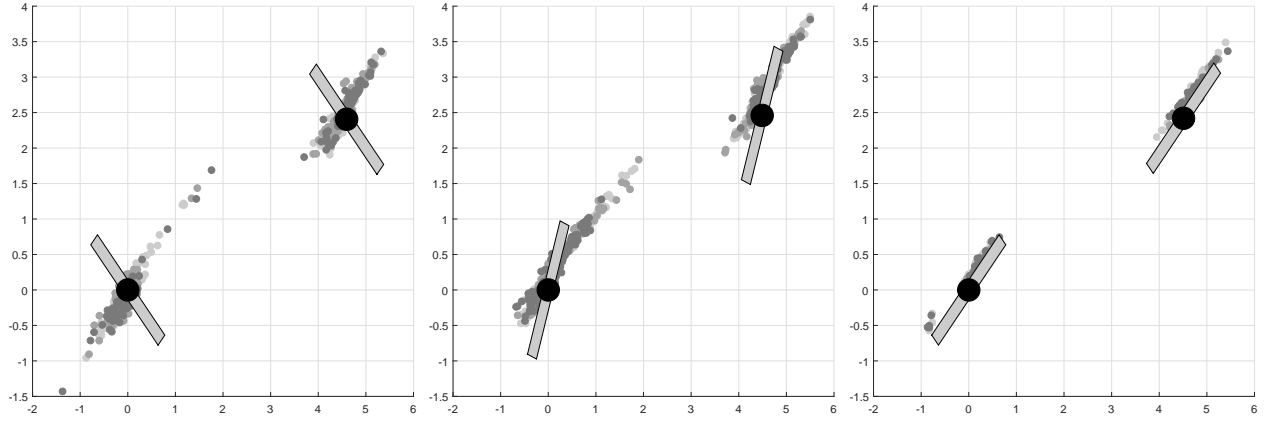

Figure 14: Results of the log recognition software. The grey dots are the estimated logs' locations using our algorithm. The black circle represents the logs' centres. The rectangular shapes represent the position of how the logs were placed for the tests. The units in these graphs are in meters.

this histogram represent the Euclidean distance for every observation in respect to the origin. In addition, the dark grey bar shows the Euclidean distance where the log was actually placed.

According to manual measurements and calculations from GNSS, the log was placed at an approximate distance of 5.2 meters from the origin (see figure 14). It is noticeable that the observations for cases a) and b) follow a normal distribution having a maximum peak around the vicinity of 5.2 meters. For the first
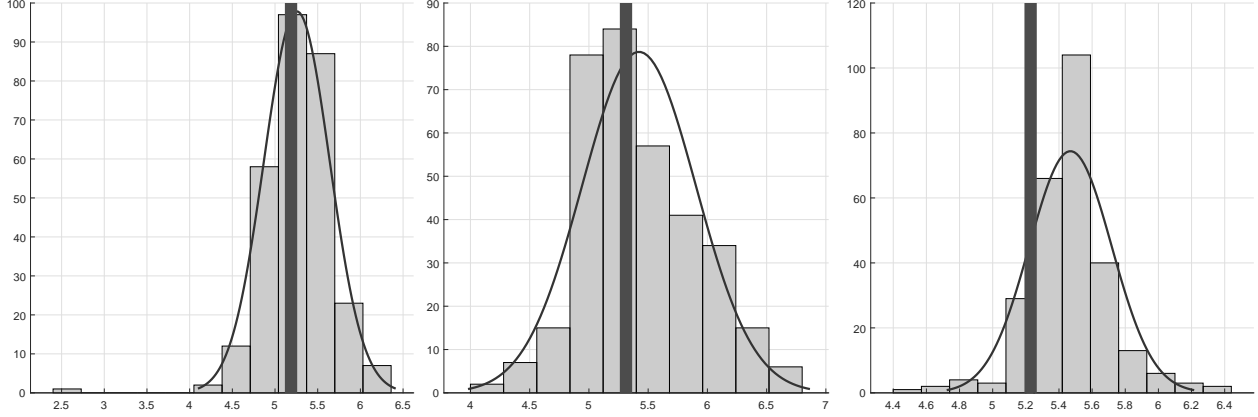
Figure 15: Results of the log recognition software using a histogram for log 2. The light grey bars represent the estimations, which clearly show a normal distribution in the vicinity of 5.2 meters. The dark grey bar represents the position where the log is actually placed.

case, measurements have an error of 3 cm, while for the second case there is an error of approximately 10 cm. However, for the case where logs are placed at a 90 degree angle, the error increases to near 30 cm. Nevertheless, due to the size of the crane's grapple, the machine will still be able to grab these logs.

Similar results for the log marked as one in figure 10 can be observed in figure 16. The location of this log represents the origin for our calculations in this particular test case. For this test, we see that for cases a) and b) the error is also within a decimetre range, while it increases to 30 cm for case c). Our results conclude that the log recognition algorithm is able to provide estimations within 10 cm of error for the cases where the camera has good visibility of the logs. The error increases to 30 cm for the worst case where camera has the minimum visibility of logs.
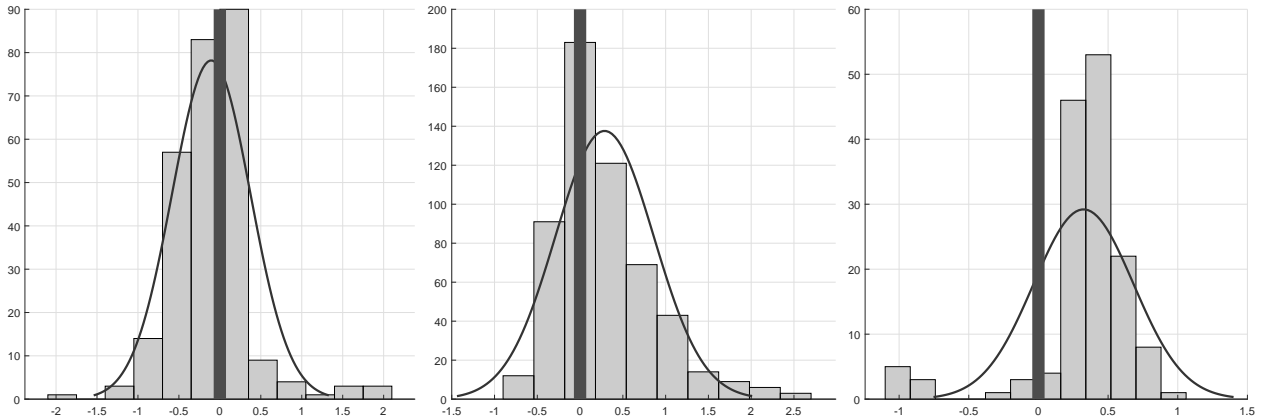

Figure 16: Results of the log recognition software using a histogram for log 1. The light grey bars represent the estimations, which clearly show a normal distribution in the vicinity of the origin. The dark grey bar represents the position where the log is actually placed.

5.1.3 Crane motion control

Referring to the tests described in section 4.1.2, figure 9 shows an example of the crane paths that our motion planning algorithm defines to move the crane towards the desired goals. For this particular test case the Cartesian coordinates for the goal positions were defined as follows: Point 1 = $[4.27, 1.86, 1]$, Point 2 = $[4.27, -1.86, 1]$, Point 3 = $[6, 1.86, 1]$, Point 4 = $[6, -1.86, 1]$.

The motions were performed multiple times to get an estimate of the crane's motion control system's accuracy. These were performed both with the grapple empty and with a load of 200 Kg. As an example, figure 17 shows data of the Cartesian coordinates of the crane tip's location for 20 tests at each testing point, i.e. 80 data points in total. The tip location was calculated by the equations of forward kinematics having values for each joint given by sensor measurements. On the left of figure 17, we show a 3D representation of the results of all tests, while the right side shows a zoomed out view of each individual point for the X-Y axis. In all the cases, the data with a square represent the motion with an empty grapple, while the data points marked with an x represent the grapple with a load of 200 Kg.
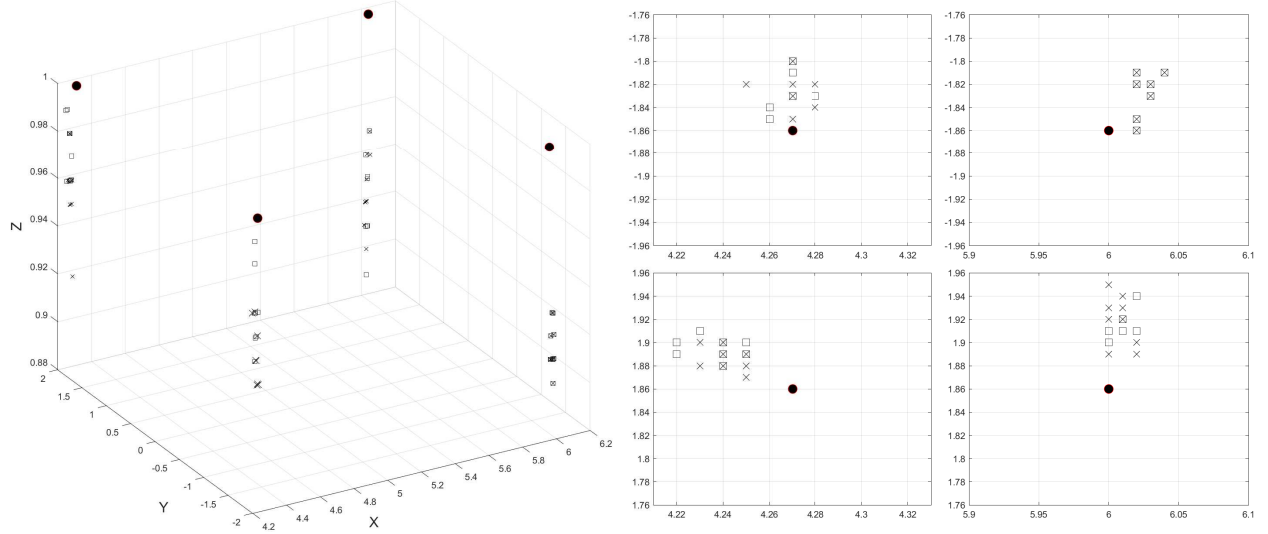

Figure 17: Example of results for each testing points. The square data points represent the grapple without load, while the x marks data points with a loaded grapple. The units for the axis in these graphs are in meters.

To show the accuracy of the crane's motion control system, we use the Euclidean distance of a data point to its desired location as a measurement of error, because this value tells how much the crane deviates from the goal location. Figure 18 presents a histogram showing these values for all data points, i.e. the data for all four desired locations are piled up into a single histogram plot. The left plot is the Euclidean distance calculated in 3D, i.e. using the data in the $[x, y, z]$ axis. The middle plot is the Euclidean distance calculated in 2D, i.e. using the data in the $[x, y]$ axis. The right plot is the error in height, i.e. z axis.

Results show that the Cartesian coordinate positioning error in 3D follows a normal distribution, having an average value of 8 cm, i.e. the crane reaches the vicinity of the desired location with an average error of 8 cm. However, we see that the error in the $[x, y]$ axis is smaller in average, i.e. 4 cm. This implies that the highest error in the crane positioning is the height of the tip, which deviates by an average of 6 cm in respect to the desired height. This phenomena can be observed in the left of figure 17, which shows that the longer the crane needs to reach the higher the deviation in the z-axis.

5.2 Testing the complete forwarding task

According to the layout presented in Figure 11, a total of 24 logs were laid out within the reach of the crane along the machine's path. Overall, 23 out of 24 logs were detected correctly. In two attempts, the detected positions had poor quality and the crane was not able to grab the logs at the optimal centre point. Table 1 shows the results from all the runs.

The effectiveness of log grasping is determined by the positioning of the log when the grapple is closed. If logs are placed beyond the maximum reach of the grapple, the attempt to grasp them will fail. However, due
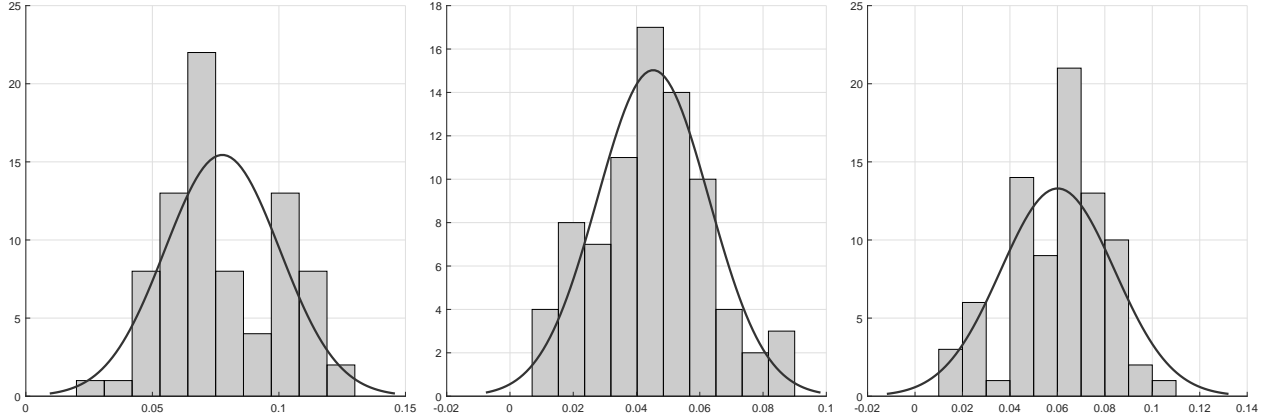
Figure 18: Cartesian positioning error for the crane's motion control system. From left to right, the histograms represent the error measured by the Euclidean distance to the desired location for 3D ([x,y,z] axis), 2D ([x,y] axis) and height (z axis), respectively.

to the large size of the grapple compared to the width of the logs, there is typically a 50 cm margin of error allowed. In the study presented in Table 1, successful attempts were defined as logs that were successfully loaded onto the trailer. In all instances where the log was successfully grasped, it was properly positioned on the loading bunk during testing.

6   Discussion

Forest industry plays an important role in the global economy and has significant influences in our lives and the environment that we live in. Therefore, considering improvements in technologies for forest harvesting is vital to secure wood supply with environmentally sound methods.

With the rapid advancements of technologies related to digitalization, automation and robotics, a transition towards more resourceful forest operations is slowly coming to fruition. Early industry adoptions of these technologies have been well received, as they provide improvements in various aspects of the work and drive the need for further advancements.

Within forestry, Scandinavian countries are well known for their high performance machinery and the research to automate them. However, despite years of developments, projects featuring full scale demonstrations with unmanned machines are rare to find in scientific literature. This makes the development shown in this article one of a kind, because it shows the practical application of combining different research areas to successfully perform fully autonomous forestry work in real world conditions. To the best of our knowledge, this is the first time that such demonstrations have taken place in the public domain, and the success on the preliminary results motivates the vision that one day fully unmanned forestry machines will be able to part take the work in forestry, as envisioned by this industry. However, there is much work to be done to achieve this goal.

The development presented in this article has centred around the introduction of an unmanned forestry machine that has been purposely built as a research platform to test advanced automation for forest operations' work. Apart of the construction of the machine, that underwent five years, we showed successful application of three key areas, i.e. autonomous navigation, log recognition via computer vision, and autonomous crane manipulation. Each of these subjects possesses its own challenge, but the initial results combining these technologies show that the accuracy of our current development is reliable enough to perform basic forwarding tasks.

Table 1: Error measured in the X and Y directions in mm (Y = machine rear longitudinal direction)

Log no.	X Error	Y Error	Z Error	Euclidian Distance Error	Successful attempt	Reason for failure
1	33,7	146,6	55,2	160,3	YES	
2	-175,9	215,8	-132,3	308,2	YES	
3	-710,8	-120,4	181,1	743,3	NO	Inaccurate estimation
4	-646,0	-23,6	-224,6	684,3	NO	Inaccurate estimation
5	-295,6	-19,9	-82,2	307,5	YES	
6	-370,2	226,7	-0,4	434,1	YES	
7	-202,7	-82,8	-9,3	219,1	YES	
8	-268,2	56,6	-79,2	285,3	YES	
9	-306,5	-181,6	-28,0	357,4	YES	
10	-292,6	222,7	-69,5	374,2	YES	
11	-100,9	88,6	70,1	151,5	YES	
12	-308,0	174,0	-42,2	356,3	YES	
13	45,8	40,1	-43,3	74,7	YES	
14	-363,6	190,5	-72,8	416,9	YES	
15	33,2	-10,9	-7,7	35,7	YES	
16	-271,3	298,0	-122,6	421,2	YES	
17	-	-	-	-	NO	CV did not detect a log
18	-120,4	70,9	-84,8	163,4	YES	
19	-191,1	-101,1	54,2	222,9	YES	
20	74,1	-8,1	-94,6	120,4	YES	
21	-402,1	-244,0	-69,0	475,4	YES	
22	-125,0	19,2	-198,4	235,3	YES	
23	-196,1	97,9	-36,3	222,1	YES	
24	-47,8	73,3	-150,3	173,9	YES	
Mean error	232,6	113,0	79,5	289,3		

6.1 Discussion about results

To perform autonomous navigation, we have currently proposed using GPS via points, as this has shown to be reliable in related industries, e.g. agriculture and mining. Our main reasoning comes from the fact that forest harvesting operations are preplanned before hand in Scandinavia. Therefore, having information about the routes for forwarding tasks is preliminary known and confirmed while the harvester is working in the forest. This allows our algorithms to have the information needed to plan GPS via points.

Using our algorithm for navigation control, we were able to demonstrate performance properties, such as exponential stability and repeatability, as the machine was able to exponentially converge towards the same path in multiple rounds, despite starting at different initial conditions and weather conditions. Although it is difficult to show the weather influence in an article, our machine has been able to perform similarly in different weather conditions and terrains. The results in this article have been from a time where the terrain was muddy due to the rain, making it difficult to drive without sliding.

A major concern in this project was the subject of computer vision, and in particular the effectiveness of the log recognition software. As this information is needed for subsequent log manipulation via crane motion control, the accuracy on the estimation of the logs' pose and location is highly important. Results show that our system is currently able to estimate logs with an averaged deviation error between 3 to 10 cm, when the camera has good visibility of the logs. This error worsens if the logs ahead of the machine are placed nearly parallel to the machine's direction of travel, because this does not let the camera observe the logs' shape properly. This result is quantitatively sufficient for our development, because logs that have been cut-to-length are much bigger in magnitude in relation to the estimation error.

Unlike industrial robot manipulators, highly accurate control of forestry cranes is challenging, due to size, weight, and hydraulic manipulator dynamics. In heavy duty hydraulic applications, we often need to make a compromise between dynamic performance and control accuracy. In these regards, our crane motion control system provides the ability to perform smooth motions with reliable accuracy. According to results, the

expected deviation from the target goal shows to be within a decimetre. However, 50% of the deviation comes from inaccurate height control(z-axis), and it is attributed to the difficulty to control height due to the length and weight of the crane, as explained in former work. Nevertheless, for forestry cranes of this magnitude (9 meters reach), the deviation error is almost negligible, and in fact it works in our advantage, because it increases the certainty that the grapple will grab logs. Therefore, considering the size of the grapple, and the size of the logs that these cranes collect, our control system does not need higher accuracy.

Our current results have several strengths. First, we were able to demonstrate autonomous navigation in a terrain that is common in forestry. Second, our results show that object recognition using machine learning can provide logs' location estimation with high accuracy for subsequent manipulation through the machine's crane. Third, our results demonstrate the feasibility of collecting logs autonomously using the crane, relying only on estimations done with the help of the camera installed in front of the machine. Four, we obtained successful results performing a fully autonomous forwarding task in an scenario that is common in clear-cut. Therefore, our system setup with minimum sensing equipment already presents the ability to carry on with forwarding tasks, because of the accuracy of algorithms developed during this project.

Despite the positive results, some limitations to our current development should be addressed. First, although we attempt to show results in real forestry conditions, our experimental environment is still idealized. So far, we have concentrated on collecting single logs, mainly to test our algorithms. Disparately, most forwarding tasks involve more complex manipulation and decision making than the ones we are using at the moment. Second, one of our objectives was to demonstrate autonomous navigation in a clear-cut terrain. To achieve this goal, our system uses DGNSS, which is available in Sweden, covering the whole nation. However, other countries might not count with similar coverage, making the AORO platform currently restricted to areas having access to DGNSS reception. In addition, a clear-cut terrain tends to have obstacles that are easy to drive over without complex obstacle avoidance methods. However, higher complexity on terrains does exist in many parts of Scandinavia and the world, and should be properly tackled with obstacle avoidance algorithms. Third, the crane's motion control currently relies on good log location and pose estimation, and it is reliable as long as deviation errors are compensated by the size of the grapple. However, to increase accuracy, the crane needs a dedicated camera which is currently not available. This would allow to further advance towards more complex manipulation, such as unloading and grabbing multiple logs.

6.2   General discussion

Automating the work of machines represents a paradigm shift in forestry. Machines in the market are already starting to exhibit automation features to facilitate the work for the operator. Upcoming developments are promising to relieved some of the work from the machines' operators hands. With the advancements in the area of robotics and automation, it is clear that this trend will continue towards removing the necessity of on-board operators. At that point, the human operator will remotely supervise the work, as it is currently done in other industries. However, there is much to be done to build an infrastructure in forestry that can meet the requirements for automation, before this vision in forestry can become a reality. In addition, development of automation technology for forestry machine is recently starting to take place.

Although we are at the early stages of making the AORO platform a system that can autonomously perform forwarding tasks, our current development demonstrates that we are reaching a point in which algorithms currently existing in robotics are robust enough to handle real world applications. Our initial results demonstrate the beginning of an unmanned machine with the ability of handling simplified work already, despite being still an ideal testing scenario.

Some of the added benefits of our development include the ability to separate the key areas of our developments in computer vision, autonomous navigation, and autonomous crane motion control. Individually, they are the essence for market products featuring semi-autonomous functions that can relief some work from machine operators' hands in the near future. However, we refrain from discussing such topic further, as this has been explained in some of our former work.

In conclusion, this article has provided an initial view of results from the AORO platform aiming at performing fully autonomous forwarding tasks. Results show that our algorithms in the key areas of computer vision, autonomous navigation, and crane motion control, meet our expected requirements in terms of accuracy and reliability. Consequently, our activity manager software is able to combine these functions to successfully perform idealized forwarding tasks in real world conditions. These results highlight the possibility that in the future, further advancements will be able to tackle forwarding tasks with comparable performance to human operators.

Acknowledgments

References

Ali, W., Georgsson, F., and Hellstrom, T. (2008). Visual tree detection for autonomous navigation in forest environment. In *2008 IEEE Intelligent Vehicles Symposium*, pages 560–565. IEEE.

AORO: Arctic Off-Road Robotics Lab (2021). Retrieved November, 2021, from https://www.skogstekniskaklustret.se/projekt/aoro.

Automated harvesting with robots in the forest (2020). Retrieved November, 2021, from https://web.fpinnovations.ca/automated-harvesting-with-robots-in-the-forest/.

Bellicoso, C. D., Gehring, C., Hwangbo, J., Fankhauser, P., and Hutter, M. (2016). Perception-less terrain adaptation through whole body control and hierarchical optimization. In *2016 IEEE-RAS 16th International Conference on Humanoid Robots (Humanoids)*, pages 558–564. IEEE.

CINTOC (Accessed on 2020). Cintoc. http://cintoc.se/.

CRANAB FC8 (2021). Retrieved November, 2021, from https://www.cranab.com/products/forwarder-cranes/fc8.

da Silva, D. Q., dos Santos, F. N., Filipe, V., Sousa, A. J., and Oliveira, P. M. (2022). Edge ai-based tree trunk detection for forestry monitoring robotics. *Robotics*, 11(6):136.

Daniel Tenezaca, B., Canchignia, C., Aguilar, W., and Mendoza, D. (2020). Implementation of dubin curves-based rrt* using an aerial image for the determination of obstacles and path planning to avoid them during displacement of the mobile robot. In *Developments and Advances in Defense and Security: Proceedings of MICRADS 2019*, pages 205–215. Springer.

Darknet: Open Source Neural Networks in C (2021). Retrieved November, 2021, from https://pjreddie.com/darknet/.

EATON (Online since 2019). https://www.eaton.com/us/en-us/catalog/valves/cma-advanced-mobile-valves.resources.html.

Eriksson, M. and Lindroos, O. (2014). Productivity of harvesters and forwarders in ctl operations in northern sweden based on large follow-up datasets. *International Journal of Forest Engineering*, 25(3):179–200.

Everingham, M., Van Gool, L., Williams, C. K., Winn, J., and Zisserman, A. (2010). The pascal visual object classes (voc) challenge. *International journal of computer vision*, 88(2):303–338.

Farhadi, A. and Redmon, J. (2018). Yolov3: An incremental improvement. In *Computer Vision and Pattern Recognition*, volume 1804. Springer Berlin/Heidelberg, Germany.

Fethi, D., Nemra, A., Louadj, K., and Hamerlain, M. (2018). Simultaneous localization, mapping, and path planning for unmanned vehicle using optimal control. *Advances in Mechanical Engineering*, 10(1):1687814017736653.

Forsyth, D. A. and Ponce, J. (2003). A modern approach. *Computer vision: a modern approach*, 17:21–48.

Fortin, J.-M., Gamache, O., Grondin, V., Pomerleau, F., and Giguère, P. (2022). Instance segmentation for autonomous log grasping in forestry operations. In *2022 IEEE/RSJ International Conference on Intelligent Robots and Systems (IROS)*, pages 6064–6071. IEEE.

Gingras, J.-F. and Charette, F. (2017). Fp innovations forestry 4.0 initiative. In *Bangor: 2017 Council on Forest Engineering Annual Meeting*.

Halme, A. and Vainio, M. (1998). Forestry robotics-why, what and when. In *Autonomous robotic systems*, pages 149–162. Springer.

Hansson, A. and Servin, M. (2010). Semi-autonomous shared control of large-scale manipulator arms. *Control Engineering Practice*, 18(9):1069–1076.

Hosseini, A., Lindroos, O., and Wadbro, E. (2019). A holistic optimization framework for forest machine trail network design accounting for multiple objectives and machines. *Canadian Journal of Forest Research*, 49(2):111–120.

Hyyti, H., Kalmari, J., and Visala, A. (2013). Real-time detection of young spruce using color and texture features on an autonomous forest machine. In *the 2013 International Joint Conference on Neural Networks (IJCNN)*, pages 1–8. IEEE.

Jelavic, E., Jud, D., Egli, P., and Hutter, M. (2021). Towards autonomous robotic precision harvesting: Mapping, localization, planning and control for a legged tree harvester. *Field Robotics*.

Johns, R. L., Wermelinger, M., Mascaro, R., Jud, D., Gramazio, F., Kohler, M., Chli, M., and Hutter, M. (2020). Autonomous dry stone. *Construction Robotics*, 4(3):127–140.

Keefe, R. F., Wempe, A. M., Becker, R. M., Zimbelman, E. G., Nagler, E. S., Gilbert, S. L., and Caudill, C. C. (2019). Positioning methods and the use of location and activity data in forests. *Forests*, 10(5):458.

Komatsu Forest AB (Online since 2017). Komatsu smartflow - new hydraulic system for forwarder. https://www.forestry.com/editorial/equipments/komatsu-smartflow-hydraulic-system-forwarder/.

La Hera, P. and Morales, D. O. (2014). Non-linear dynamics modelling description for simulating the behaviour of forestry cranes. *International Journal of Modelling, Identification and Control*, 21(2):125–138.

La Hera, P., Morales, D. O., and Mendoza-Trejo, O. (2021). A study case of dynamic motion primitives as a motion planning method to automate the work of forestry cranes. *Computers and Electronics in Agriculture*, 183:106037.

La Hera, P. and Ortíz Morales, D. (2015). Model-based development of control systems for forestry cranes. *Journal of Control Science and Engineering*, 2015.

Lawal, M. O. (2021). Tomato detection based on modified yolov3 framework. *Scientific Reports*, 11(1):1–11.

Li, S. and Lideskog, H. (2021). Implementation of a system for real-time detection and localization of terrain objects on harvested forest land. *Forests*, 12(9):1142.

Lideskog, H., Karlberg, M., and Bergsten, U. (2015). Development of a research vehicle platform to improve productivity and value-extraction in forestry. *Procedia CIRP*, 38:68–73.

Lindroos, O., La Hera, P., and Häggström, C. (2017). Drivers of advances in mechanized timber harvesting–a selective review of technological innovation. *Croatian Journal of Forest Engineering: Journal for Theory and Application of Forestry Engineering*, 38(2):243–258.

Lindroos, O., Mendoza-Trejo, O., La Hera, P., and Ortiz Morales, D. (2019). Advances in using robots in forestry operations. In University of Southern Queensland, Australia and Billingsley, J., editors, *Burleigh Dodds Series in Agricultural Science*, pages 233–260. Burleigh Dodds Science Publishing.

Liu, M., Han, Z., Chen, Y., Liu, Z., and Han, Y. (2021). Tree species classification of lidar data based on 3d deep learning. *Measurement*, 177:109301.

Lundbäck, M., Häggström, C., and Nordfjell, T. (2021). Worldwide trends in methods for harvesting and extracting industrial roundwood. *International Journal of Forest Engineering*, 32(3):202–215.

Lundmark, H., Josefsson, T., and Östlund, L. (2017). The introduction of modern forest management and clear-cutting in sweden: Ridö state forest 1832–2014. *European Journal of Forest Research*, pages 1–17.

Manner, J., Mörk, A., and Englund, M. (2019). Comparing forwarder boom-control systems based on an automatically recorded follow-up dataset. *Silva Fenn*, 53:10161.

Manring, N. D. (2005). *Hydraulic Control Systems*. John Wiley & Sons, New York, USA, first edition.

Morales, D. O., La Hera, P., Westerberg, S., Freidovich, L. B., and Shiriaev, A. S. (2014). Path-constrained motion analysis: An algorithm to understand human performance on hydraulic manipulators. *IEEE Transactions on Human-Machine Systems*, 45(2):187–199.

Münzer, M. E. (2004). *Resolved motion control of mobile hydraulic cranes*. Aalborg University, Institute of Energy Technology.

Nguyen, H. T., Lopez Caceres, M. L., Moritake, K., Kentsch, S., Shu, H., and Diez, Y. (2021). Individual sick fir tree (abies mariesii) identification in insect infested forests by means of uav images and deep learning. *Remote Sensing*, 13(2):260.

Nordfjell, T., Öhman, E., Lindroos, O., and Ager, B. (2019). The technical development of forwarders in sweden between 1962 and 2012 and of sales between 1975 and 2017. *International Journal of Forest Engineering*, 30(1):1–13.

Nurminen, T., Korpunen, H., and Uusitalo, J. (2006). Time consumption analysis of the mechanized cut-to-length harvesting system.

Oliveira, L. F., Moreira, A. P., and Silva, M. F. (2021). Advances in forest robotics: A state-of-the-art survey. *Robotics*, 10(2):53.

Ortiz Morales, D., Westerberg, S., La Hera, P. X., Mettin, U., Freidovich, L., and Shiriaev, A. S. (2014). Increasing the level of automation in the forestry logging process with crane trajectory planning and control. *Journal of Field Robotics*, 31(3):343–363.

Pagnussat, M., Hauge, T., Silva Lopes, E. d., Martins de Almeida, R. M., and Naldony, A. (2020). Bimanual motor skill in recruitment of forest harvest machine operators. *Croatian Journal of Forest Engineering: Journal for Theory and Application of Forestry Engineering*, 41(1):25–33.

Park, Y., Shiriaev, A., Westerberg, S., and Lee, S. (2011). 3d log recognition and pose estimation for robotic forestry machine. In *2011 IEEE International Conference on Robotics and Automation*, pages 5323–5328. IEEE.

Phiquepal, C., Orthey, A., Viennot, N., and Toussaint, M. (2022). Path-tree optimization in discrete partially observable environments using rapidly-exploring belief-space graphs. *IEEE Robotics and Automation Letters*, 7(4):10160–10167.

Purfürst, F. T. (2010). Learning curves of harvester operators. *Croatian Journal of Forest Engineering: Journal for Theory and Application of Forestry Engineering*, 31(2):89–97.

Rack mountable Simulink/RTW target, ideal for HIL applications (2021). Retrieved November, 2021, from https://www.ueidaq.com.

Rånman, H. (2015). Utveckling av kontaktorgan till terrängdrönare.

Reitz, J., Schluse, M., and Roßmann, J. (2019). Industry 4.0 beyond the factory: An application to forestry. In *Tagungsband des 4. Kongresses Montage Handhabung Industrieroboter*, pages 107–116. Springer.

Roslan, Z., Awang, Z., Husen, M. N., Ismail, R., and Hamzah, R. (2020). Deep learning for tree crown detection in tropical forest. In *2020 14th International Conference on Ubiquitous Information Management and Communication (IMCOM)*, pages 1–7. IEEE.

Salton, G. and McGill, M. J. (1983). *Introduction to modern information retrieval*. mcgraw-hill.

Shorten, C. and Khoshgoftaar, T. M. (2019). A survey on image data augmentation for deep learning. *Journal of Big Data*, 6(1):1–48.

Sihvo, S., Virjonen, P., Nevalainen, P., and Heikkonen, J. (2018). Tree detection around forest harvester based on onboard lidar measurements. In *2018 Baltic Geodetic Congress (BGC Geomatics)*, pages 364–367. IEEE.

Spong, M., Hutchinson, S., and Vidyasagar, M. (2006). *Robot Modeling and Control*. John Wiley and Sons, New Jersey.

Technion (Online since 2017). Crane control systems. https://technion.fi/crane-control-systems/.

The death of the forest Beast (2006). Retrieved November, 2021, from https://www.forest-monitor.com/en/death-forest-beast/.

The Mathworks (Online since 1990). http://www.mathworks.com.

The radio-controlled bio-energy harvester forest ebeaver (2011). Retrieved November, 2021, from http://ebeaver.se/Default.aspx.

The world's first self-propelled forestry machine (2021). Retrieved November, 2021, from https://gamingsym.in/the-worlds-first-self-propelled-forestry-machine-removes-man-from-the-equation/.

Unmanned ground vehicles for the most demanding conditions (2021). Retrieved November, 2021, from https://rakkatec.com.

Visser, R. and Obi, O. F. (2021). Automation and robotics in forest harvesting operations: Identifying near-term opportunities. *Croatian Journal of Forest Engineering: Journal for Theory and Application of Forestry Engineering*, 42(1):13–24.

Wells, L. A. and Chung, W. (2023). Real-time computer vision for tree stem detection and tracking. *Forests*, 14(2):267.

Westerberg, S. (2014). *Semi-automating forestry machines: motion planning, system integration, and human-machine interaction*. PhD thesis, Umeå Universitet.

Wu, J., Yang, Q., Bao, G., Gao, F., et al. (2009). Algorithm of path navigation line for robot in forestry environment based on machine vision. *Nongye Jixie Xuebao= Transactions of the Chinese Society for Agricultural Machinery*, 40(7):176–179.

Yarak, K., Witayangkurn, A., Kritiyutanont, K., Arunplod, C., and Shibasaki, R. (2021). Oil palm tree detection and health classification on high-resolution imagery using deep learning. *Agriculture*, 11(2):183.

YOLO ROS: Real-Time Object Detection for ROS (2021). Retrieved November, 2021, from https://github.com/leggedrobotics/darknet-ros.

Zoto, J., Musci, M. A., Khaliq, A., Chiaberge, M., and Aicardi, I. (2020). Automatic path planning for unmanned ground vehicle using uav imagery. In *Advances in Service and Industrial Robotics: Proceedings of the 28th International Conference on Robotics in Alpe-Adria-Danube Region (RAAD 2019) 28*, pages 223–230. Springer.